Tectonometamorphic discontinuities in the Greater Himalayan Sequence: a local or a regional feature?

Tectono-metamorphic discontinuities in the Greater Himalayan Sequence, a local or a regional feature?

Chiara Montomoli [(1)]*, Rodolfo Carosi[(2)], Salvatore Iaccarino [(1)]

[(1)] Dipartimento di Scienze della Terra, v. S. Maria, 53 56126 Pisa, Italy

[(2)] Dipartimento di Scienze della Terra, v. Valperga Caluso, 35 10125 Torino, Italy

* Corresponding author: (email: chiara.montomoli@unipi.it)

number of words of text and references:

number of tables: 1

number of figures: 4

Abbreviated title: Discontinuities in the GHS

Formatted

Abstract

The Greater Himalayan Sequence is one of the major tectonic units of the Himalayas running for over than 2400 km along strike. It has been considered as a coherent tectonic unit bounded by the South Tibetan Detachment and the Main Central Thrust. However thrusts within it have been recognized in several places and have been mainly interpreted as out of sequence thrusts being active after the main phase of exhumation of the crystalline unit constrained after the activation of the MCT. Recent integrated studies allow to recognise several ductile shear zones in the core of the GHS along the belt, with top-to-the SW sense of shear (Higher Himalayan Discontinuity). U-Th-Pb in situ monazite ages provide ages older than the Main Central Thrust. Data on the P and T evolution testify that these shear zones affected the tectono-metamorphic evolution of the belt and different P and T conditions were recorded in the hanging-wall and footwall of the Higher Himalayan Discontinuity. The correlation of the HHD with other discontinuities recognized in the GHS led to propose that it is a tectonic feature running for several hundreds kilometers, documented at the regional scale dividing the GHS in two different portions.

Key words: Himalaya, tectonic discontinuities, metamorphic discontinuities, Greater Himalayan Sequence, shear zone.

Several first-order tectonic discontinuities have been recognized in the Himalayas dividing the main tectonic units, such as from top to bottom: the South Tibetan Detachment (STD), the Main Central Thrust (MCT), the Main Boundary Thrust (MBT) and the Main Frontal Thrust (MFT). The spectacular continuity of these structures and the main tectonic units for more than 2400 km, in between them, is a unique feature of the Himalayan belt.

The Greater Himalayan Sequence (GHS) is one of these main tectonic units building up the chain, bounded by the upper STD and the lower MCT from respectively the Tethyan Sedimentary Sequence (TSS) and the Lesser Himalayan Sequence (LHS). It represents the metamorphic core of the belt and medium to high-grade metasedimentary, meta-igneous rocks and Miocene granites constitute it. Even if it has been undergone a complex deformation history a quite uniform and coherent tectonic - lithostratigraphy has been recognized all along strike (Le Fort 1971, 1975; Searle & Godin 2003, Yin 2006).

So far researchers paid attention to the meaning of the MCT, its spectacular continuity along the belt and its role in the collisional and post-collisional evolution. In the eighties the

identification of the upper tectonic boundary of the GHS as a normal fault and moreover its contemporaneity with the MCT, shed new light on the tectonic evolution of the belt leading to the formulation of different tectonic models for the exhumation of the GHS. Models span from rigid extrusion, ductile extrusion by simple shear, non-coaxial ductile extrusion, channel flow and channel flow followed by extrusion (for a review see Mukherjee 2013, Mukherjee & Koyi 2010, Mukherjee *et al*. 2012 and Montomoli *et al*. 2013). Most of the current tectonic models proposed till now for the exhumation of the GHS are exclusively based on the role of the first order discontinuities (MCT and STD) and most of the studies concentrated on these tectonic boundaries.

Several tectonic discontinuities have been recognized inside the GHS located in different structural positions and usually interpreted as out-of-sequence thrusts (Mukherjee *et al*., 2012) such as the Kalopani and the Modi Khola shear zones in Central Nepal (Vannay & Hodges 1996; Hodges *et al*. 1996), the Kakhtang and Laya thrusts in Bhutan (Daniel *et al*. 2003; Grujic *et al*. 2012), the Tamor-Khola Thrust in far-eastern Nepal (Schelling & Arita, 1991) and the Trisuli-Likhu Fault in the Kathumandu Nappe, central Nepal (Arita *et al.* 1997). According to Mukherjee *et al.* (2012) it is a unique out of sequence thrust localized at various levels in the GHS (distance ratio of the out of sequence thrust from the MCT and the STDS varying from 1:0.25 to 1:1.57)

A number of ductile shear zones localized within the core of the GHS in Nepal Himalayas were active before the activation of the Main Central Thrust (Carosi *et al*. 2010; Montomoli *et al*. 2103 with references). Moreover a growing evidence of the occurrence of a main horizon in the GHS where these ductile shear zones develop led to recognize the occurrence of first order tectonic discontinuity along the belt dividing the GHS in two portions with different P-T-t paths (Larson *et al*. 2010; Montomoli *et al*. 2013; Yakymchuk & Godin 2012).

By the way a main problem arises in correlating these discontinuities along the belt as they have been recognized using different criteria such as: a) structural criteria using kinematic indicators and high-strain concentration (Goscombe *et al.* 2006; Carosi *et al*. 2010; Montomoli *et al*. 2013; Larson *et al*. 2013); b) detecting different P-T (Groppo *et al*. 2009; Yakymchuk & Godin 2012), c) P-T-t paths from hanging-wall and footwall rocks (Corrie & Khon 2011; Imayama *et al*. 2010, 2012) and d) in a few cases just determining different geochronological ages from hanging-wall and footwall (Rubatto *et al*. 2012).

Multidisciplinary studies, based on meso and microstructural analyses, in situ U-Th-Pb geochronology and P-T paths on the hanging-wall and footwall rocks, showed that the GHS is divided into two main portions or sub-units (GHS lower – GHS_l and GHS upper – GHS_u,

Yakymchuk & Godin 2012) separated by a tectono-metamorphic discontinuity identified as the Higher Himalayan Discontinuity (HHD) (Carosi *et al*. 2010; Montomoli *et al*. 2013). Its occurrence affects both the tectonic and the metamorphic evolution of the GHS being active before the onset of the MCT and causing the earlier exhumation of the GHS_u at least in Western Nepal (Carosi *et al*. 2010; Montomoli *et al*. 2013).

The aim of this work is to make a review of the discontinuities recognized inside the GHS (Fig. 1) and to check their possible correlation along the Himalayan belt in order to assess the occurrence of a regional tectonic feature and to better characterize the structural setting of the GHS.

Geological setting

The Himalayan mountain chain is regarded as the most classical example of continental related collision. Since a long time (Heim & Gansser 1939) three main tectonic units have been recognized all along the belt (Fig. 1).

These tectonic units from bottom to top are: (i) Lesser Himalayan Sequence, (ii) Greater Himalayan Sequence and (iii) Tethyan Sedimentary Sequence. They are bounded by northward dipping orogenic scale tectonic discontinuities, such as the upper South Tibetan Detachment (Burchfiel *et al*. 1992, Carosi *et al*. 1998) and the lower Main Central Thrust (Gansser 1964; Searle *et al*. 2008). These tectonic units have been formerly deposited on the Indian passive margin and later deformed during the India–Asia collision started about 55 Ma (Searle *et al.* 1987; Hodges 2000 and references therein).

The lowermost tectonic unit in the orogenic pile (Lesser Himalayan Sequence, LHS) is made by very-low grade to lower amphibolite facies metamorphic rocks (Upreti 1999; Hodges 2000) mainly represented by impure quartzite, marble, phyllites, orthogneiss and metamafic rocks. The LHS is subdivided in two groups (Upreti 1999), separated by an unconformity: (i) the "Lower Lesser Himalaya", made by Paleo-Protorezoic to Meso-Proterozoic sedimentary rocks and orthogneiss and (ii) the "Upper Lesser Himalaya" made by sedimentary rocks of middle Proterozoic age, unconformably overlain by rocks of Gondwanan affinity of Upper Paleozoic to Cenozoic in age.

The GHS, tectonically overlays the LHS, *via* a km wide top-to-the-South shear zone, named Main Central Thrust Zone (MCTZ), is constituted by a 20-30 km thick sequence of medium to high-grade metasedimentry and meta-igneous rocks. The GHS is subdivided into three different lithotectonic units (Le Fort 1971, 1975; Searle & Godin, 2003). The lowermost unit

(Unit 1) is constituted by metasedimentary rocks mainly represented by Ky-bearing paragneiss and micaschist with subordinate calc-schists, quartzite, impure marble and migmatites upward. Above, Unit II, is a sequence made mainly by calcsilicate gneiss and marbles with minor pelitic and psammitic rocks. The upper portion of the GHS is made by orthogneiss and sillimanite-bearing migmatitic rocks (Unit III). Most of the GHS protoliths are metasediments Neoproterozoic to Late Cambrian in age with lower Paleozoic intrusions (Hodges, 2000).

One peculiarity of the GHS is the presence at its base of an inverted metamorphic field gradient, with the highest metamorphic grade rocks structurally above the lowest grade ones (Gansser 1964; Searle & Rex 1989). Along the belt the structural thickness of the GHS is quite variable, reaching minimum values of 2-3 km in western Nepal (Carosi *et al.* 2002, 2007) up to 30 km in Eastern Nepal and Bhutan (e.g. Daniel *et al*. 2003).

The metamorphic rocks of the GHS are intruded by Oligo-Miocene granites (Visonà *et al*. 2012, Searle 2013). These granites are mainly subdivided into two groups (i) two mica ± tourmaline leucogranite and (ii) tormaline leucogranite, yielding U-Th-Pb monazite and U-Pb zircon ages spanning from 24-19 Ma (Searle & Godin 2003; Carosi *et al*. 2013) with few younger leucogranites between 14 and 7 Ma (Leech 2008; Kellet *et al*. 2010). Whereas most of the leucogranites are intruded in the GHS and are deformed in the ductile portion of the STDS, an undeformed granite has been recently found in western Nepal with the peculiar characteristics of cross cutting the STDS, intruding both GHS and TSS at about 24-23 Ma (Bertoldi *et al*. 2011, Carosi *et al*. 2013).

The uppermost tectonic unit is the Tethyan Sedimentary Sequence (TSS), tectonically above the GHS through a top-to-the- North ductile to brittle extensional structures, named the South Tibetan Detachment System (Burchfiel *et al*. 1992).

The TSS is composed by Cambrian to Eocene marine sediments from non-metamorphic to deformed under very-low to low-grade metamorphic conditions (Antolin *et al*. 2011; Dunkl *et al*. 2011; Crouzet *et al.* 2007; Myrow *et al.* 2009). To the North the TSS is bounded by the Indus Yarlung Suture Zone (Fig. 1), made by flyschs and ophiolites derived from the Neotethys Ocean (Hodges 2000).

Discontinuities in the Greater Himalayan Sequence

The GHS has been considered for a long time as a coherent tectonic unit. Anyway several discontinuities have been highlighted in different structural positions in the metamorphic core, striking parallel to the belt.

The first recognized tectonic discontinuities have been interpreted as out-of –sequence thrusts (Grujic *et al*. 1996, 2002; Hodges *et al*. 1996; Vannay & Hodges 1996; Davidson *et al*. 1997; Searle 1999; Viskupic & Hodges 2001; Daniel *et al.* 2003) being active after the main phase of exhumation of the crystalline unit constrained after the activation of the MCT (see Mukherjee *et al.* 2012 for a review).

These discontinuities are mainly characterized by mineral lineations trending perpendicular to the grain of the belt and put in contact hanging wall (HW) and footwall (FW) rocks characterized by different metamorphic imprints, such as for example the Kakhgtang thrust in Bhutan (Grujic *et al*. 1996; Daniel *et al*. 2003) or the Modi Khola shear zone in Central Nepal (Hodges *et al*. 1996).

Even if most of the discontinuities show orogen-perpendicular mineral lineations, recently in southern Tibet, gently dipping shear zones with penetrative orogen-parallel mineral lineations have been recognized in the upper portion of the GHS (Xu *et al.* 2013). They show both top-to-the-East and top-to-the-West sense of movement but occurred later than MCT activity (Xu *et al.* 2013).

The tectonic discontinuities in the GHS in Western Nepal, active before the MCT and with consequences on the metamorphic evolution of the upper and lower GHS (*i.e.* on the P-T-t paths of the HW and FW), have been identified as the HHD following Montomoli *et al*. (2013).

This is a primary tectonic feature in Western Nepal and we concentrate on similar tectonic-metamorphic discontinuities in other sections of the belt with the aim to check the regional extent of the HHD.

Since previous Authors used different criteria to identify discontinuities in the GHS such as structural criteria, metamorphic criteria, geochronological criteria and/or combination among them, we analyse and discuss the possible correlation criteria with the HHD reported in the literature.

Tectonic and metamorphic discontinuities (P-T-t-D discontinuities)

Recently multidisciplinary studies led to recognize a HHD (Montomoli *et al*. 2013) located in the core of the GHS. Along two different sections of the belt, in Western Nepal, the integration of structural data, P-T estimations and geochronological datings led to recognize a major tectonic and metamorphic discontinuity in the GHS (Carosi *et al*. 2010, Montomoli *et al*. 2013).

According to Montomoli *et al.* (2013) along the westernmost transect (Mugu Karnali) (Fig. 1) the HHD is a ductile contractional shear zone (Mangri Shear Zone, MSZ) with a thickness of 4 km affecting paragneiss, micaschist, migmatitic gneiss and orthogneiss deformed from protomylonites to mylonites. Kinematic indicators (represented mainly by C-S fabric, rotated asymmetric porphyroclasts, micafishes and minor drag folds) show a top-to-the SW sense of shear (Fig. 2a, b, c, e and e). Mineral lineations trend from NE-SW to ENE-WSW and plunge 30-40° toward the NE.

The shear zone developed during the decompression, in the sillimanite stability field, of rocks that previously underwent relatively high-pressure metamorphism deformed in the kyanite stability field. Along the mylonitic foliation synkinematic growth of sillimanite can be observed (Fig. 2f), accompanied by high-temperature deformation mechanism in quartz, such as chessboard extinction (Fig. 2d).

P-T paths estimated for samples coming from the HW and FW revealed quite similar peak temperatures (FW: 650-700°C and HW: 690-720°C) but a break of pressure array in correspondence of the shear zone. More in detail the shear zone juxtaposes lower pressure rocks (~0.7-0.8 GPa) above higher pressure rocks (~1.1-0.9 GPa) with a pressure gap of nearly 0.2 GPa (Fig. 3, Table 1).

In situ dating, performed through U-(Th)-Pb on monazite on samples from HW and FW, revealed different ages for rocks from different structural position (i.e. HW and FW). In particular in situ geochronological techniques, paired with microstructural observations and correlation of different chemical domains in monazites with metamorphic reactions and /or deformation events, led to recognize a continuous activity of the shear zone between 25 and 18 Ma (Table 1). Deformation ages have been obtained on monazites, sometimes with sillimanite inclusions, aligned along the mylonitic sillimanite bearing foliation.

The HHD crops out eastward and affects kyanite bearing paragneiss and micaschist with subordinate calc-silicate and marble in the FW and sillimanite bearing gneiss and micaschist and migmatite in the HW (Toijem Shear Zone, TSZ, Carosi *et al.* 2010) (Fig. 1). Mineral lineations trend NE-SW and plunge 30-40° towards the NE. Kinematic indicators (C –S - C' fabric, mica fishes, rotated asymmetric porphyroclasts) point to a top – to - the SW sense of shear. P-T paths indicate that the FW experienced higher pressure (0.9 GPa) than the HW (0.7 GPa) and reached temperatures in the range of 675-700°C for HW rocks and in the range of 600-650°C for FW rocks (Fig. 3). Shear zone activity has been constrained through in situ analyses on monazite. Geochronological data highlighted that the shear zone was active from ~ 26 Ma and ended at ~ 17 Ma (Table 1).

A structural and metamorphic break referred as Nyalam Thrust (NT) was recently recognized by Wang *et al*. (2013), in the Nyalam area (South-Central Tibet, Fig. 1) in correspondence of a pressure reversion of *c.* 0.3 GPa. The NT juxtaposes high - grade sillimanite (+ K-feldspar) to cordierite-bearing migmatitic gneiss (hanging wall) above the lower, slightly mylonitized rocks, mainly made by non-migmatized Ky/Sil (+ muscovite) paragneiss and orthogneiss (footwall). According to Wang *et al.* (2013) kinematic indicators show a top-to-the-South sense of shear and lineations moderatly dip to the NNE. A detailed P-T profile is reported by Wang *et al.* (2013), revealing a broadly decrease of pressure at "peak temperature" up section, in the FW rocks and roughly in HW rocks.
In FW rocks package, P-T conditions range from *c.* 650-670 °C and 1.3-0.9 GPa of structurally lower Ky gneiss up to c. 670°C -0.49-0.38 GPa for Sil-bearing rocks just below the NT. In the HW rocks P-T estimates vary from c. 705-750°C and 0.41-0.70 GPa. The timing of shearing of the NT is very poorly constrained, but Wang *et al.* (2013) using zircon U-Pb ages, suggested an age for NT shearing younger than 14 Ma, postdating the movement along STDS and MCT in that region (their Fig. 11).

A P-T-t-D discontinuity has been recognized by Larson *et al.* (2013) in Eastern Nepal, in the Tama Kosi region (Fig. 1). In this area the HW is made by kyanite-sillimanite bearing gneiss while the FW is constituted by staurolite bearing micaschist and paragneiss. Different P-T paths characterize the HW and FW rocks. The HW reached P-T conditions of 700°- 750°C and 1.0- 0.7 GPa while the FW rocks reached temperature of 620°C and pressure of 0.7 GPa The FW rocks reached peak metamorphic conditions at ~10 Ma, in contrast HW rocks record an earlier and protracted prograde metamorphic history (>21Ma) and started to be decompressed at c. 19 Ma and likely continuing until c. 15 Ma (Larson *et al*. 2013).
This discontinuity has been interpreted as a boundary between hinterland and foreland of the belt and approximately corresponds to the MCT.
Recently, in the same geological transect, a structurally upper discontinuity, within the sillimanite grade rocks, has been reported by Larson & Cottle (2014), based on the variation of temperature detected by quartz fabric (Fig. 3, Table 1).
Metamorphic monazite U-Th-Pb ages of the HW sample are basically identical with ages reported by Larson *et al.* (2013) for the FW sample (retrograde conditions < 22Ma), suggesting a post metamorphic peak activity for such discontinuity, but at higher temperature deformation regime and still older than the lower ones (c. 22 Ma vs 19-15 Ma., Fig. 10 in Larson & Cottle, 2014).

In Central Nepal, in the Himal Chuli area (Fig. 1) a discontinuity is located between sillimanite bearing, locally anatectic, gneiss from the lower staurolite and kyanite bearing metasedimentary rocks with minor igneous intercalations and quartzite, calcsilicate schist, marble and pelitic schist (Larson *et al.* 2010).

HW and FW rocks were deformed under the same temperature range (~600-650°C) but experienced notably different peak pressure and while the HW rocks reached 0.5-0.4 GPA the FW rocks reached 0.9-1.1 GPa (Fig. 3, Table 1). Peak metamorphic conditions have been achieved in an interval range between 23 and 15 Ma (Table 1).

In Eastern Nepal (Fig. 1) another top-to-the-South, ductile shear zone has been described by Goscombe *et al*. (2006) called High Himal Thrust (HHT). This discontinuity is a 100-400 m thick, high-strain mylonitic zone, reworking the high-grade migmatitic GHS rocks, with synkinematic growth of biotite, feldspar and sillimanite. It divides the GHS into two portions named respectively Upper Plate and Lower Plate characterized by different P-T-t-D histories (Table 1). The Upper Plate (HW) is mainly composed by migmatitic rocks with upper amphibolite to granulitic metamorphic rocks and Miocene leucogranitic intrusion.

The Lower Plate (FW) is made by rocks with an inverted metamorphic grade, varying from biotite to partially molten metamorphic rocks (Goscombe *et al*. 2006, Imayama *et al*. 2010, 2012). Moreover, the strain recorded by the HW (strain ratio: 3-10) is typically lower than the strain recorded in the FW (strain ratio: 4-20).

Imayama *et al*. (2010, 2012) constrained the P-T-t evolution of this discontinuity (Table 1).

The migmatites in the hanging wall record partial melting (0.7-1.0 GPa, 730-780 °C) at c. 33-28 Ma and melt crystallization on cooling at 27-23 Ma, while the migmatites in the footwall record the starting of partial melting (0.8-1.4 GPa, 720- 770°C) at Early Miocene (21-18 Ma) followed by melting cooling around 18-16 Ma (Imayama *et al.* 2012). Moreover, these two portions of GHS have two different average cooling rates, with the hanging wall rocks testifying a slower cooling rate (15-25 °C/Ma) compared with the footwall (30-40 °C/Ma) (Imayama *et al.* 2012). These observations support the first role of High Himal Thrust, and diachronic equilibration of the GHS rocks in Eastern Nepal. Goscombe *et al*. (2006) also reported a very late reactivation of HHT as a normal fault.

Metamorphic discontinuities

Many discontinuities have been recognized in Nepal Himalayas mainly detecting different P-T evolutions from rocks in the HW and in the FW. We refer to them as metamorphic discontinuities.

Yakymchuk & Godin (2012) recognized a metamorphic discontinuity (MD) in the far-northwest Nepal (Fig. 1). The MD separates the GHS_u characterized by kyanite and sillimanite bearing migmatitic gneisses from the GHS_l dominated by staurolite and kyanite bearing micaschist with subordinate quartzite, calcsilicate schist, augen orthogneiss and amphibolite. The GHS_l is characterized by an inverted metamorphic gradient and roughly correspond to the MCT zone.

The MD, previously interpreted as the MCT (Robinson *et al*. 2006), is a metamorphic discontinuity dividing two tectonometamorphic domains, the lower one characterized by an increase in peak metamorphic temperature and pressures up section (1.1 GPa and 600-630°C), while the upper one shows a decrease in metamorphic pressures at peak temperatures up-section (0.6-0.8 GPa and 650-720°C) (Fig. 3, Table 1). The juxtaposition of the two tectono-metamorphic domains requires significant displacement so that the Authors proposed that the discontinuity represents both a metamorphic and a tectonic discontinuity.

In Central Nepal, in the Annapurna massif (Fig. 1), two different metamorphic discontinuities have been recognized in the lower portion of the GHS both of them located in the Unit 1 (Searle & Godin 2003) by Corrie & Kohn (2011). The lower metamorphic discontinuity (Bhanuwa Thrust) divides the lower portion of Unit 1 made by kyanite bearing micaschist from the intermediate portion of the unit constituted by rocks with the same metamorphic assemblage but locally migmatized. Monazite ages give 24-17 Ma for the activity of the discontinuity. The ages of the high Y monazites rim, interpreted as retrograde, in the hanging wall could constrain the activity of the Bhanuwa Thrust, triggering their retrograde path, at nearly 22 -17 Ma. This discontinuity has been interpreted by the Authors as the MCT.

The upper metamorphic discontinuity (Sinuwa Thrust), in between the lower kyanite bearing poorly migmatitic pelitic rocks (with average T-P condition of 735°C and 1.25 GPa) from the upper kyanite bearing pervasively migmatitic pelitic rocks (with an average of "peak P-T" condition at 775°C and 12.5 GPa) is well constrained through Th-Pb ages of monazites giving a range of 27-23 Ma for its activity (Table 1).

Metamorphic "hidden" discontinuities have been recognized by Groppo *et al*. (2009) in Eastern Nepal (Ama Drime Range) (Fig. 1).

They identified, from different P-T paths, a lower and an upper discontinuity at different structural levels in the GHS. In particular they localized the two discontinuities in the Main Central Thrust Zone (MCTZ) affecting the GHS.

The lower discontinuity is between chlorite and garnet bearing micaschist in the FW (T=550°C, P:0.65 GPa) and staurolite and kyanite bearing micaschist in the HW (T=600-650°C, P:0.85- 0.95 GPa). This discontinuity has been interpreted as the lower limit of the MCTZ, corresponding to the MCT *sensu* Heim & Gansser (1939).

The upper Hidden Discontinuity ("Hidden Discontinuity" in Table 1) is localized between staurolite and kyanite bearing micaschist in the FW and kyanite and sillimanite bearing migmatites in the HW. FW rocks are characterized by higher pressure values (about 0.95 GPa) with respect to the HW rocks (0.75 GPa) (Fig. 3) so that in absence of structural data the Authors interpreted this discontinuity as an extensional contact as it juxtaposes lower pressure rocks above higher pressure ones.

In Central Nepal (Langtang Section) (Fig. 1) Inger & Harris (1992), and Harris & Massey (1994) proposed a discontinuity corresponding to the sillimanite/kyanite isograd diving the GHS in an upper portion of sillimanite bearing rocks (with relict of kyanite), from a lower one made by kyanite bearing rocks. Inger & Harris (1994) proposed a diachronous evolution between kyanite and sillimanite bearing rocks and Fraser *et al.* (2000), using high-precision geothermobarometry, recognized two different crustal portions, as a result of post-metamorphic juxaposition of two different thrust sheets. Reddy *et al.* (1993) even if they did not report P-T data, along the same geological transect, argued for a structural break between kyanite and sillimanite bearing rocks using microstructural and isotopic observations.

Geochronological constraints on the P-T-t evolution in the Langtang section are presented by Kohn *et al.* (2004, 2005) and Kohn (2008). From the latter authors it is evident how the upper portion of the GHS (named Langtang Thrust Sheet by Kohn *et al.* 2004) and the lower portion of GHS (Main Central Thrust Sheet of Kohn *et al.* 2004) underwent similar P-T reactions history, but in different times, with the uppermost rocks being metamorphosed (and melted) and than exhumed/cooled several Ma before the lowermost ones (*e.g.* Fig. 2 in Kohn *et al.* 2004), although the boundary between the two crustal slices do not strickly coincide with Ky-Sil transition.

Rubatto *et al.* (2012), in the Sikkim region (Eastern Himalaya) (Fig. 1), documented two different tectonic slices of GHS integrating petrology and trace element-constrained U-Pb geochronology. The higher structural portion reached peak metamorphic conditions (and melting) several million years (~5 Ma) after respect to the lower strucural level (Table 1). In order to explain the diachronicity in the metamorphic and melting history of the GHS, Rubatto *et al.* (2012) claimed for a discontinuity between the two portions ("Age

discontinuity" in Table 1). This discontinuity has been further confirmed by Sorcar *et al.* (2014) on the basis of a different petrologic cooling rate between hanging-wall and footwall.

More to the East (Fig. 1), in Bhutan, Swapp & Hollister (1991) identified a discontinuity in the core of the GHS between the lower staurolite and kyanite bearing micaschist and paragneiss and the upper sillimanite + k-feldspar ± cordierite bearing migmatite ("Bhutan Thrust" in Table 1). The FW rocks underwent 480-500°C and 0.7 GPa while HW rocks reached 630°C and much lower pressure values around 0.4 GPa (Swapp & Hollister 1991). Even in absence of geochronological data the Authors suggest that the proposed discontinuity predated the last motion on the Main Central Thrust because it occurred at higher temperature compared to the deformation temperature of most of the rocks along the MCT in Bhutan.

Discussion

The GHS has been regarded for a very long time as a coherent tectonic unit. The widespread uniform $^{40}Ar/^{39}Ar$ cooling ages of white micas (Vannay & Hodges 1996) reinforced the intepretation of the GHS as a unique tectonic unit. The "uniform" cooling ages of a particular minerals (*e.g* argon-argon ages of micas) especially for not texturally controlled ages (Mulch & Cosca 2004), should be taken with caution since the juxtaposition of crustal blocks could have been occurred during higher-temperature deformation regime, well above the mineral closure temperature. So that, the GHS could have behaved as a coherent tectonic unit only during the latest stages of exhumation and cooling (Rubatto *et al.* 2012).

By the way several tectonic discontinuities in the GHS have been recognized along the Himalayan belt from western Nepal to Bhutan, through Sikkim and Eastern and Central Nepal. Some discontinuities, such as the "Bhanuwa Thrust" (Corrie & Kohn 2011), the lower "Tama Kosi P-T-t-d discontinuity" (Larson *et al.* 2013) and the lower discontinuity of Groppo *et al.* (2009) correspond in fact to the Main Central Thrust and are localized at the base of the GHS. The other discontinuities, localized within the GHS above the Main Central Thrust Zone, divide the GHS into two portions: an upper one (Upper Greater Himalayan Sequence- GHS_u) and a lower one (Lower Greater Himalayan Sequence- GHS_l).

In general, as the discontinuities have been recognized using different criteria (structural, metamorphic, geochronologic or a combination of them), their correlation sometimes is not so obvious. Anyway, in spite of the different used criteria, they show some common features

A common feature is that the HW rocks (GHS_u) are usually sillimanite or kyanite bearing migmatite, or partially molten rocks, showing a higher degree of melting with respect to the FW rocks (GHS_l).

It is worth to note that different P-T paths have been highlighted for FW and HW and in most of the cases HW rocks are characterized by lower pressure values than the FW rocks (Fig. 3).

Where structural criteria have been applied, kinematic indicators show that tectonic discontinuities are characterized by a top-to-the South-South West sense of movement. Mylonitic foliation is characterized by the syn-kinematic growth of high-temperature minerals, such as sillimanite.

Some discontinuities, such as the Kakhtang and Laya Thrusts in Bhutan (Grujic *et al*. 1996; Grujic *et al*. 2012) and Nyalam Thrust in Nepal (Mukherjee *et al.* 2012; Wang et *al*. 2013), are active between 15 and 10 Ma. The other discontinuities (Table 1) are older and are active in a time interval of several Myr, starting their activity from ≈ 27- 26 Ma (Carosi *et al.* 2010; Imayama *et al.* 2012). While the first younger ones can be interpreted as out of sequence thrusts the older ones should be considered in sequence thrusts.

Taking into account all the common aspects of the recognized discontinuities we can correlate them across the belt and we can address for a regional extent of the HHD (Fig. 1, Table 1). By the way some remarks are necessary considering the different criteria used to distinguish the discontinuities. Using only metamorphic criteria or P-T differences from HW and FW rocks without the direct observation of kinematic indicators can led to erroneous interpretations preventing a reliable sense of movement. As a consequence, even the same metamorphic discontinuity has been interpreted both as contractional or normal sense shear zone (i.e. Corrie & Kohn 2011 versus Martin *et al*. 2010 for the HHT in Eastern Nepal).

The common assumption that lower pressure metamorphic rocks are tectonically juxtaposed over higher pressure ones only by a normal fault can be misleading in the case in which rocks attitude dips more than that of tectonic discontinuity but in the same direction. In this case a thrust can be responsible for their superposition (Twiss & Moores 1992).

Moreover, kinematic indicators, where observed, indicate a top-to-the-South contractional shear zone. Only in the HHT a normal reactivation of the shear zone has been detected (Goscombe *et al.* 2006, Imayama *et al.* 2012)

The contractional HHD started to move during the underthrusting of the GHS and while the footwall rocks continued to be buried, the hanging wall rocks underwent earlier exhumation. As a consequence, the peak P-T conditions reached by HW and FW rocks during

the activity of the HHD are diachronous. In addition to this we can find along the same vertical section the superposition of lower P rocks over higher P ones.

If we consider only the P-T-t paths, without the exact deformation path of the deformed rocks or, at least, the geometry and kinematic indicators in the mylonites, we could erroneously interpret the HHD to be a normal sense shear zone (in contrast to the movement indicated by kinematic indicators) because relatively lower pressure rocks occur in the hanging wall (Carosi *et al.* 2010).

The correlation between the metamorphic index minerals from different structural positions (e.g. bottom and top of GHS) may be equally problematic as it is necessary to know if they grew during prograde or decompression paths and if the index mineral represents time/spatial variation of "thermal peak" attainment due differences in bulk rock composition or to different P-T-t-D history of the rock packages.

The occurrence of a regional-scale discontinuity within the GHS suggests that it is made by at least two crustal slices with different P-T-t histories. Whatever their coupling mechanism, the occurrence of folded isograds connecting index minerals between the lower and the upper crustal slices, required for example by channel flow model (Searle & Szulc 2005), is unlikely.

A fundamental support to investigate this problem is to study :

1) microstructures with the relations between index minerals and main foliations

2)relations between microstructures and the timing of fabric acquisition via *in situ* geochronology (monazite and others accessories mineral growth)

Montomoli *et al.* (2013) showed that deformation shifted in space and time from the HHD to the lower MCT. A problem arises because ductile deformation in shear zones localizes strain in a thick portion of the GHS with variable thickness. When a shear zone accommodating dozen or hundreds km of displacement works for several Myr it could widen its boundaries both to the bottom and to the top because of strain hardening within its core. The shear zone boundaries can broaden at the point to meet or to merge with the deformation linked to the upper (and older) discontinuity. Example of this behaviour could be the HHD almost coincident with the upper boundary of the MCTZ proposed by Goscombe *et al*. (2006), Yakymchuk & Godin (2012) and Larson *et al*. (2013)

However a correct identification of the two shear zones (HHD vs MCT) and to univocally characterize tectonic discontinuities is to use a multidisciplinary approach joining structural,

456 metamorphic and geochronological investigations for both HW and FW rocks and high strain
457 zone (Carosi *et al*. 2010; Goscombe *et al*. 2006; Larson *et al*. 2013; Montomoli *et al.* 2013).
458
459 **HHD and metamorphism in the GHS**
460
461 The activity of the HHD starting form 27-26 Ma affected also the metamorphic history of the
462 rocks of the GHS causing a diachronicity of the P-T peak conditions in the rocks separated by
463 the HHD (Fig. 4). Following collision at ~55 Ma the GHS underwent general prograde
464 metamorphism. The structural, metamorphic and geochronological data on the HW and FW
465 of the HHD allow to identify the retrograde path of the HW rocks corresponding to the
466 exhumation caused by the top-to-the SW and thrust-sense shearing at 27-18 Ma of the HHD
467 (Montomoli *et al.* 2013 with references therein). Ductile deformation in the HW of the HHD
468 ceased as documented by undeformed leucogranite dykes cross cutting the ductile fabric
469 emplaced at 17 Ma (Carosi *et al.* 2010). When deformation localized at a lower level in the
470 FW of the HHD (*i.e.* MCT), thrust-sense shearing allowed the HW of the MCT (the FW of the
471 HHD) to change its P-T-t path and to exhume. The exhumation path is triggered by activation
472 of the MCT at 17-13 Ma in Western Nepal (Montomoli *et al*. 2013).
473 This shows that, in Western Nepal, deformation at nearly 17 Ma shifted from the HHD to a
474 lower discontinuity in the GHS that can be identified with the MCT zone.
475 All these data support a downward and southward progressive migration of deformation
476 (not only limited to the MCTZ and LHS as proposed by previous Authors such as Searle *et al.*
477 2008) and ductile shearing within the GHS allowing the progressive exhumation of crustal
478 slices of the GHS.

479 The activity of the HHD can explain the occurrence of higher T in the HW with respect to the
480 FW by the positive inflection of isotherms in the HW and negative inflection in the FW
481 caused by the thrust-sense movement (Fig. 4). From the sketch of Fig. 4 it is expected the
482 HW rocks undergo decompression and decreasing temperature. If we take into
483 consideration the natural P-T-t paths of HW rocks it is evident a slightly increase in
484 temperature during the decompression path of nearly ~50°-100°C (Carosi *et al.* 2010;
485 Groppo *et al.* 2009; Montomoli *et al*. 2013).

486 This increasing temperature, compared to peak temperature during the decompression
487 path, could be explained by the addition of shear heating along the HHD. The temperature
488 increase during exhumation path could be due to radioactive heating occurring in the GHS,

causing partial melting due to U, Th and K present in the rocks (Faccenda *et al*. 2008; Nábělek & Nábělek 2014).

According to Molnar and England (1990) heating due to friction on a low-angle thrust fault, like the MCT, at a depth of 15-20 km is in the order of ~ 100°C. According to Mukherjee and Mulchrone (2012) shear heating is more efficient in extruding rocks where deformation is close to simple shear as it is common in high-strain shear zones at depth.

The HHD is a regional-scale discontinuity, developing for hundreds kilometres along strike, affecting the evolution of the GHS since 27-26 Ma not easily explained by the current tectonic models adopted for the GHS. In fact, most of them such as extrusion, channel flow, wedge insertion and even critical taper (see Montomoli *et al.* 2013 for a review) or a combination of critical taper and channel flow (Mukherjee 2013), are based on the contemporaneous activity of the upper STDS and the lower MCT (active between 23-17 Ma, Godin *et al.* 2006) or even if they do not require their simultaneous activity, STDS and MCT have always a primary role.
In addition to this the timing of metamorphism and deformation in the GHS is not contemporaneous as required by models based on the contemporaneous STD-MCT activities but the two crustal slices (GHS upper and lower) show differences in the timing of deformation and metamorphism with a southward shifting of both of them.
Updated tectonic models of the evolution and exhumation of the GHS should take into account the regional occurrence of the HHD and its impact to the exhumation of the core of the Himalayas.

Conclusion

The wide regional occurrence of compressive in sequence ductile tectonic discontinuities, from Western Nepal to Sikkim, and their relative ages distribution, both along the belt and across a vertical section of the GHS affected the tectonic and metamorphic evolution of the GHS (Carosi *et al.* 2010, 2013; Imayama *et al.* 2012; Montomoli *et al.* 2013).
A regional tectonic-metamorphic discontinuity (HHD) has been recognized in the GHS with the following characteristics:
- it is a ductile shear zone showing a contractional top-to-the S and SW sense of shear;

- it divides the GHS in two portions; an upper GHS and a lower GHS. The upper GHS is made of sillimanite-kyanite migmatites with a high-degree of melting whereas the lower GHS is mainly made by rocks exhibiting a lower degree of melting ;
- the HHD started its activity before the initiation of the MCT, at 27-26 Ma and continued up to 17 Ma;
- the HW and FW rocks attained peak metamorphic conditions in different times. The FW attained peak metamorphism later than the HW;
- the HW often registered lower P at "peak temperature" with respect to the FW;
- the HW underwent exhumation before MCT and STD activities.

The actual proposed models of exhumation based mainly on the MCT and STD activities are not able to explain the occurrence of the HHD and the difference in the timing of metamorphism between GHS_u and GHS_l. Any model of the tectonic evolution of the GHS should account for the occurrence of the HHD and its consequences on the metamorphic path.

Acknowledgments

This work is dedicated to the memory of our colleague and friend Bruno Lombardo remembering his passion and love for Himalayan geology and all our fruitful discussion.
Research funded by PRIN 2010-2011 and Funds ex-60% Universities of Pisa and Torino (C. Montomoli, R. Carosi). Review from T. Imayama and S. Mukherjee greatly improved the manuscript. We warmly thank Angharad Hills and Rick Law for support from the Geological Society of London.

References:

Antolín, B., Appel, A., Montomoli, C., Dunkl, I., Ding, L., Gloaguen, R. & El Bay, R. 2011. Kinematic evolution of the eastern Tethyan Himalaya: constraints from magnetic fabric and structural properties of the Triassic flysch in SE Tibet. *In*: Poblet, J., & Lisle, R. (eds.) *Kinematic Evolution and Structural Styles of Fold-and-Thrust Belts.* Geological Society of London Special Publications, **349**, pp. 99–121.

Arita, K., Dallmeyer, R. D. & Takasu, A., 1997. Tectonothermal evolution of the Lesser Himalaya, Nepal: Constraints from 40Ar/39Ar ages from the Kathmandu Nappe. *The Island Arc*, **6**, 372-385.

Bertoldi, L., Massironi, M., Visonà, D., Carosi, R., Montomoli, C., Gubert, F., Naletto, G. & Pelizzo, M.G., 2011. Mapping the Buraburi granite in the Himalaya of Western Nepal: remote sensing analysis in a collisional belt with vegetation cover and extreme variation of topography. *Remote Sensing of Environment*, **115**, 1129-1144.

Burchfiel, B.C., Chen Z., Hodges, K.V.; Liu Y., Royden, L.H., Changrong, D., Xu, L., 1992. The South Tibetan Detachment System, Himalayan Orogen: Extension contemporaneous with and parallel to shortening in a collisional mountain belt. *Geological Society of America Special Paper*, **269**, 1-41.

Carosi, R., Lombardo, B., Molli G., Musumeci, G. ,Pertusati, P.C., 1998. The South Tibetan Detachment System in the Rongbuk valley, Everest region. Deformation features and geological implications. *Journal of Asian Earth Sciences*, **16**, 299-31

Carosi, R., Montomoli, C. & and Visonà, D. 2002. Is there any detachment in the Lower Dolpo (western Nepal)? *Comptes Rendus Geoscience*, ***334***, 933–940.

Carosi, R., Montomoli, C. & Visonà, D. 2007. A structural transect in the Lower Dolpo: insights on the tectonic evolution of Western Nepal. *Journal of Asian Earth Sciences,* **29**, 407–423.

Carosi, R., Montomoli, C., Rubatto, D. & Visonà, D. 2010. Late Oligocene high-temperature shear zones in the core of the Higher Himalayan Crystallines (Lower Dolpo,Western Nepal). *Tectonics*, **29**, TC4029, http://dx.doi.org/10.1029/2008TC002400.

Carosi, R., Montomoli, C., Rubatto, D. & Visonà, D. 2013. Leucogranite intruding the South Tibetan Detachment in western Nepal: implications for exhumation models in the Himalayas. *Terra Nova*, **25**, 478-489, doi: 10.1111/ter.12062.

587 Catlos, E. J., Dubey, C. S., Harrison, T. M., & Edwards M. A. 2004. Late Miocene movement
588 within the Himalayan Main Central Thrust shear zone, Sikkim, north-east India. *Journal of*
589 *Metamorphic Geology*, **22**, 207–226.
590
591 Chambers, J., Parrish, R., Argles, T. & Harris, N. 2011. A short-duration pulse of ductile
592 normal shear on the outer South Tibetan detachment in Bhutan: alternating channel flow
593 and critical taper mechanics of the eastern Himalaya. *Tectonics*, **3**, TC2005.
594
595 Corrie, S. L. & Kohn, M. J. 2011. Metamorphic history of the Central Himalaya, Annapurna
596 region, Nepal, and implication for tectonic models. *Geological Society of American Bulletin*,
597 **123**, 1863–1879.
598
599 Crouzet, C., Dunkl, I., Paudel, L., Arkai, P., Rainer, T. M., Balogh, K. & Appel, E. 2007.
600 Temperature and age constraints on the metamorphism of the Tethyan Himalaya in Central
601 Nepal: a multidisciplinary approach. *Journal of Asian Earth Sciences*, **30**, 113–130.
602
603 Daniel, C. G., Hollister, L., Parrish, R. R. & Grujic D. 2003. Exhumation of the Main Central
604 thrust from lower crustal depths, Eastern Bhutan Himalaya. *Journal of Metamorphic Geology*,
605 **21**, 317–334.
606
607 Davidson, C., Grujic, D., Hollister, L., & Schmid, S.M., 1997. Metamorphic reaction related to
608 decompression and synkinematic intrusion of leucogranite, High Himalayan Cristallines,
609 Bhutan. *Journal of Metamorphic Geology*, **15**, 593–612.
610
611 DeCelles, P. G., Robinson, D. M., Quade, J., Ojha, T., Garzione, C., Copeland, P. & Upreti B. N.
612 2001. Stratigraphy, structure, and tectonic evolution of the Himalayan fold thrust belt in
613 western Nepal. *Tectonics*, **20**, 487–509, doi:10.1029/2000TC001226
614 Dunkl, I., Antolín, B., Wemmer, K., Rantitsch, G., Kienast, M., Montomoli, C., Ding, L., Carosi, R.,
615 Appel, E., El Bay, R., Xu, Q. & von Eynatten, H. 2011. Metamorphic evolution of the Tethyan
616 Himalayan flysch in SE Tibet. *In*: Gloaguen, R., & Ratschbacher, L. (eds.), *Growth and Collapse*
617 *of the Tibetan Plateau*. Geological Society of London Special Publications, **353**, pp. 45–69.
618

619

620 Faccenda, M., Gerya, T. V. & Chakraborty, S. 2008. Styles of post-subduction collisional
621 orogeny: Influence of convergence velocity, crustal rheology and radiogenic heat production.
622 *Lithos*, **103**, 257–287.

623 Fraser, G., Worley, B. & Sandiford, M. 2000. High-precision geothermobarometry across the
624 High Himalayan metamorphic sequences, Langtang valley, Nepal. *Journal of Metamorphic*
625 *Geology*, **18**, 665–685.
626

627 Gansser, A. 1964. Geology of the Himalayas. *New York Wiley Interscience*, 289 pp.
628

629 Godin, L., Grujic, D., Law, R. D. & Searle, M. P. 2006. Channel flow, ductile extrusion and
630 exhumation in continental collision zones: an introduction. *Geological Society of London*
631 *Special Publication,* **268**, 1–23.
632

633 Goscombe, B., Gray, D. & Hand, M. 2006. Crustal architecture of the Himalayan metamorphic
634 front in eastern Nepal. *Gondwana Research*, **10**, 232–255.
635

636 Groppo, C., Rolfo, F. & Lombardo, B., 2009. P–T evolution across the Main Central Thrust
637 Zone (Eastern Nepal): hidden discontinuities revealed by petrology. *Journal of Petrology*, **50**,
638 1149–1180.
639

640 Grujic, D. 2006. Channel flow and continental collision tectonics: an overview. In: Law R. D.,
641 SearleM. P. & Godin L. (eds.) *Channel Flow, Ductile Extrusion and Exhumation in Continental*
642 *Collision Zones*. Geological Society of London Special Publication, **268**, 25-37.
643

644 Grujic, D., Casey, M., Davidson, C., Hollister, S. L., Kündig, R., Pavlis, T. & Schmid, S. 1996.
645 Ductile extrusion of the Higher Himalayan Crystalline in Bhutan: evidence from quartz
646 microfabrics. *Tectonophysics*, **260**, 21–43.
647

648 Grujic, D., Hollister, L. S. & Parrish R. R. 2002. Himalayan metamorphic sequence as an
649 orogenic channel: insight from Bhutan. *Earth and Planetary Sciencs Letters*, **198**, 177-191.
650

651 Grujic, D.,Warren, C. J. & Wooden, J. L. 2012. Rapid synconvergent exhumation of
652 Mioceneaged lower orogenic crust in the eastern Himalaya. *Lithosphere*, **3**, 346–366.
653
654 Harris, N. & Massey, J. 1994. Decompression and anatexis of Himalayan metapelites.
655 *Tectonics*, **13**, 1537–1546.
656
657 Heim, A. & Gansser, A. 1939. Central Himalaya: a geological observations of the Swiss
658 expedition 1936. *Memoirs of the Swiss Society of Natural Sciences*, **73**, p. 245.
659
660 Hodges, K. V., Parrish, R. R., & Searle M. P. 1996. Tectonic evolution of the central
661 AnnapurnaRange, Nepalese Himalayas. *Tectonics*, **15**, 1264-1291.
662
663 Hodges, K. V. 2000. Tectonics of the Himalaya and southern Tibet from two perspectives.
664 **746**, *Geological Society of America bullettin*, **112**, 324-350.
665 Hubbard, M.S. & Harrison,T.M. 1989. 40Ar/39Ar Age constraints on deformation and
666 metamorphism in the main central thrust zone and tibetan slab, eastern Nepal Himalaya.
667 *Tectonics*, **8**, 4, 865-880.
668
669 Imayama, T., Takeshita, T. & Arita, K. 2010. Metamorphic P–T profile and P–T path
670 discontinuity across far-eastern Nepal Himalaya: investigation of channel flow models.
671 *Journal of Metamorphic Geology*. **28**, 527–549.
672
673 Imayama, T., Takeshita, T., Yi, K., Cho, D.-Y., Kitajima, K., Tsutsumi, Y., Kayama, M., Nishido, H.,
674 Okumura, T., Yagi, K., Itaya, T. & Sano, Y., 2012. Two-stage partial melting and contrasting
675 cooling history within the Higher Himalayan Crystalline Sequence in the far-eastern Nepal
676 Himalaya. *Lithos* **134–135**, 1–22.
677
678 Inger, S. & Harris, N. B. W. 1992. Tectonothermal evolution of the High Himalayan crystalline
679 sequence, Langtang Valley, northern Nepal. *Journal of Metamorphic Geology*, **10**, 439–452.
680

681 Kellett, D. A., Grujic, D., Warren, C., Cottle, J., Jamieson, R. & Tenzin, T. 2010. Metamorphic
682 history of a syn-convergent orogen parallel detachment: the South Tibetan detachment
683 system, Bhutan Himalaya. *Journal of Metamorphic Geology*, **28**, 785–808.
684
685 Kohn, M. J. 2008. P-T-t data from Nepal support critical taper and repudiate large channel
686 flow of the Greater Himalayan Sequence. *Geological Society of America Bulletin*, **120**, 259–
687 273.
688
689 Kohn, M. J., Catlos, E., Ryerson, F. J. & Harrison, T. M. 2001. Pressure-Temperature-time path
690 discontinuity in the Main Central thrust zone, Central Nepal. *Geology*, **29**, 571-574.
691
692 Kohn, M. J., Wielnand, M., Parkinson, C. D. & Upreti, B. N. 2004. Miocene faulting at plate
693 tectonic velocity in the Himalaya of central Nepal. *Earth and Planetary Science Letters*, **228**,
694 299–310.
695
696 Kohn, M. J., Wielnand, M., Parkinson, C. D. & Upreti, B. N. 2005. Five generation of monazite in
697 Langtang gneisses: implication for chronology of the Himalayan metamorphic core. *Journal*
698 *of Metamorphic Geology*, **23**, 399–406.
699
700 Larson, K. P. 2012. The geology of the Tama Kosi and Rolwaling valley region, East-Central
701 Nepal. *Geosphere*, **8**, 507-517.
702
703 Larson, K. P., & Cottle, J. M. 2014. Midcrustal Discontinuities and the Assembly of the
704 Himalayan mid-crust. *Tectonics*, DOI: 10.1002/2013TC003452 in press.
705
706 Larson, K. P., Cottle, J. M. & Godin, L. 2011. Petrochronologic record of metamorphism and
707 melting in the upper Greater Himalayan sequences, Manaslu–Himal Chuli Himalaya, west-
708 central Nepal. *Lithosphere*, **3**, 379–392.
709
710 Larson, K. P., Gervais, F. & Kellett, D. A. 2013. A P–T–t–D discontinuity in east-central Nepal:
711 Implications for the evolution of the Himalayan mid-crust. *Lithos*, **179**, 275–292.
712

713 Larson, K. P., Godin, L. & Price, R. A. 2010. Relationships between displacement and
714 distortion in orogens: linking the Himalayan foreland and hinterland in central Nepal.
715 *Geological Society of American Bulletin*, **122**, 1116–1134.
716
717 Le Fort, P. 1971. Les formations cristallophyliennes de la Thakkhola. *Recherches géologiques*
718 *dans l'Himalaya du Népal, région del Thakkhola*, Édition du CNRS Paris.
719
720 Le Fort, P. 1975. Himalaya: the collided range. *American Journal of Science,* **275A**, 1-44.
721 Leech, M. L, 2008. Does the Karakoram fault interrupt mid-crustal channel flow in the
722 western Himalaya? *Earth and Planetary Science Letters*, **276**, 314–322.
723
724 Long, S. P. & McQuarrie, N. 2010. Placing limits on channel flow: insights from the Bhutan
725 Himalaya. *Earth and Planetary Science Letters*, **290**, 375–390.
726
727 Macfarlane, A. M. 1993. Chronology of tectonic events in the crystallines core of the
728 Himalaya, Langtang, National Park, central Nepal. *Geological Society of America Bulletin*, **104**,
729 1389–1402.
730
731 Martin, A. J., Ganguly, J. & DeCelles, P. G. 2010. Metamorphism of Greater and Lesser
732 Himalayan rocks exposed in the Modi Khola valley, central Nepal. *Contributions to*
733 *Mineralogy and Petrology*, **159**, 203–223.
734
735 Molnar, P. & England, P., 1990. Temperature, Heat Flux and Frictional Stress Near Major
736 Thrust Faults. *Journal of Geophysical Research*, **95**, 4833-4856.
737
738 Montomoli, C., Iaccarino, S., Carosi, R., Langone, A. & Visonà, D. 2013. Tectonometamorphic
739 discontinuities within the Greater Himalayan Sequence in Western Nepal (Central
740 Himalaya): Insights on the exhumation of crystalline rocks. *Tectonophysics*, **608**, 1349-1370,
741 doi:10.1016/j.tecto.2013.06.006.
742
743 Mulch, A. & Cosca M. A. 2004. Recrystallization or cooling ages: in situ UV-laser $^{40}Ar/^{39}Ar$
744 geochronology of muscovite in mylonitic rocks. *American Mineralogist*, 161, 573-582.
745

Mukherjee, S. 2011. Mineral fish: their morphological classification, usefulness as shear sense indicators and genesis. *International Journal of Earth Sciences*, **100**, 1303-1314.

Mukherjee, S 2013. Channel flow extrusion model to constrain dynamic viscosity and Prandtl number of the Higher Himalayan Shear Zone. *International Journal of Earth Sciences,* **102**, 1811-1835.

Mukherjee, S & Koyi, HA (2010). Higher Himalayan Shear Zone, Sutlej section: structural geology and extrusion mechanism by various combinations of simple shear, pure shear and channel flow in shifting modes. *International Journal of Earth Sciences,* **99**, 1267-1303.

Mukherjee, S. & Mulchrone, K. 2013. Viscous dissipation pattern in incompressible Newtonian simple shear zones: an analytical model. *International Journal of Earth Sciences,* **102**, 1165-1170

Mukherjee, S., Koyi, H.A., & Talbot, C. 2012. Implications of channel flow analogue models for extrusion of the Higher Himalayan Shear Zone with special reference to the out-of-sequence thrusting. *International Journal of Earth Sciences (Geol. Rundsch.)*, **101**, 253-272.

Myrow, P. M., Hughes, N. C., Searle, M. P., Fanning, C. M., Peng, S. C. & Parcha, S. K. 2009. Stratigraphic correlation of Cambrian–Ordovician deposits along the Himalaya: implications for the age and nature of rocks in the Mount Everest region. *Geological Society of America Bulletin*, **121**, 323–332.

Nábělek, P. I. & Nábělek J. L. 2014. Thermal characteristics of the Main Himalaya Thrust and the Indian lower crust with implications for crustal rheology and partial melting in the Himalaya orogen. *Earth and Planetary Science Letters*, **395**, 116–123.

Nadin, E. S. & Martin, A. J. 2012, Apatite thermochronometry within a knickzone near the Higher Himalaya front, central Nepal: No resolvable fault motion in the past one million years. *Tectonics*, **31**, TC2010, doi:10.1029/2011TC003000.

778 Reddy, S. P., Searle, M. P. & Massey, J. A. 1993. Structural evolution of the High Himalayas
779 gneiss sequences, Langatang Valley, Nepal. *In*: Treloar, P.J. & Searle, M.P. (eds.), *Himalayan*
780 *Tectonics*, Special Publications, vol. 7. The Geological Society, London, pp. 375–389.
781
782 Robinson, D. M., DeCelles, P.G., & Copeland, P. 2006. Tectonic evolution of the Hiamalayan
783 thrust belt in western Nepal: implications for channel flow models. *Geological Society of*
784 *American Bulletin*, **118**, 865-885.
785
786 Rubatto, D., Chakraborty, S. & Dasgupta, S. 2012. Timescale of crustal melting in the Higher
787 Himalayan Crystallines (Sikkim, Eastern Himalaya) inferred from trace element-constrained
788 monazite and zircon chronology. *Contributions to Mineralogy and Petrology*, **165**, 349-372,
789 http://dx.doi.org/10.1007/s00410-012-0812-y.
790
791 Schelling, D. & Arita, K., 1991. Thrust tectonics, crustal shortening, and the structure of the
792 far-eastern Nepal Himalaya. *Tectonics*, **10**, 5, 851-862.
793
794 Searle, M. P. 1999. Extensional and compressional faults in the Everest–Lhotse Massif,
795 Khumbu Himalaya, Nepal. *Journal of the Geological Society of London,* **156**, 227–240.
796
797 Searle, M. P. 2013. Crustal melting, ductile flow and deformation in mountain belts: cause
798 and effect relationships. *Litosphere,* **5**, 547-554.
799
800 Searle, M. P. & Godin, L. 2003. The South Tibetan Detachment System and the Manaslu
801 Leucogranite: a structural reinterpretation and restoration of the Annapurna–Manaslu
802 Himalaya, Nepal. *Journal of Geology*, **111**, 505–523.
803
804 Searle, M. P., & Rex, A. J. 1989. Thermal model for the Zanskar Himalaya. *Journal of*
805 *Metamorphic Geology*, **7**, 127–134, doi: 10.1111/j.1525-1314.1989.tb00579.x,
806
807 Searle, M. P., & Szulc, A. G. 2005. Channel flow and ductile extrusion of the high Himalayan
808 slab-the Kangchenjunga–Darjeeling profile, Sikkim Himalaya. *Journal of Asian Earth Sciences*,
809 **25**, 173-185.
810

811 Searle, M. P., Law, R. D., Godin, L., Larson, K., Streule, M.J., Cottle, J. M. & Jessup, M. J. 2008.
812 Defining the Himalayan Main Central Thrust in Nepal. *Journal of the Geological Society of*
813 *London*, **165**, 523–534, http://dx.doi.org/10.1144/0016-76492007-081.
814
815 Searle M. P., Windley, B. F. & Coward, M. P. 1987. The closing of Tethys and tectonics of the
816 Himalaya. *Geological Society of America Bulletin*, **98**, 127-134.
817
818 Sorcar, N., Hoppe, H., Dasgupta, S. & Chakraborty, S. 2014. High-temperature cooling
819 histories of migmatites from the High Himalayan Crystallines in Sikkim, India: rapid cooling
820 unrelated to exhumation? *Contribution to Mineralogy and Petrology*, **167**, 957 DOI
821 10.1007/s00410-013-0957-3.
822
823 Spear, F. S., Kohn, M. J. & Cheney, J. T. 1999. P-T path from anatectic pelites. *Contribution to*
824 *Mineralogy and Petrology*, **134**, 17-32.
825
826 Swapp, S. M. & Hollister, S. 1991. Inverted metamorphism within the Tibetan slab of Bhutan:
827 evidence for a tectonically transported heat sources. *Canadian Mineralogist*, **29**, 1019–1041.
828
829 Tobgay, T., McQuarrie, N., Long, S., Kohn, M. J. & Corrie, S. L. 2012. The age and rate of
830 displacement along the Main Central Thrust in the western Bhutan Himalaya. *Earth and*
831 *Planetary Science Letters*, **319-320**, 146-158.
832
833 Twiss, R. J. & Moores, E. M. 1992. Structural Geology. W.H. Freeman and Company (eds.).
834 532 pp. ISBN 0-7167-2252-6.
835
836 Upreti, B.N. 1999. An overview of the stratigraphy and tectonics of the Nepal Himalaya.
837 *Journal of Asian Earth Sciences*, **17**, 577–606.
838
839 Vannay, J. C. & Hodges, K. V. 1996. Tectonometamorphic evolution of the Himalayan
840 metamorphic core between the Annapurna and Dhaulaghiri, Central Nepal. *Journal*
841 *of Metamorphic Geology*, **14**, 635–656.
842

Viskupic, K. & Hodges, K. V. 2001. Monazite-xenotime thermochronometry: methodology and an example from the Nepalese Himalaya. *Contribution to Mineralogy and Petrology*, **141**, 233-247.

Viskupic, K, Hodges, K. V., & Bowring S. A. 2005. Timescales of melt generation and the thermal evolution of the Himalayan metamorphic core, Everest region, eastern Nepal. *Contribution to Mineralogy and Petrology*, **149**, 1–21.

Visonà, D., Carosi, R., Montomoli, C., Peruzzo, L. & Tiepolo, M. 2012. Miocene andalusite leucogranite in central-east Himalaya (Everest–Masang Kang area): low-pressure melting during heating. *Lithos*, **144**, 194–208.

Wang, J. M., Zhang, J. J., & Wang, X. X., 2013. Structural kinematics, metamorphic P-T profiles and zircon geochronology across the Greater Himalayan Crystalline Complex in south-central Tibet: implication for a revised channel flow. *Journal of Metamorphic Geology*, **31**, 607-628.

Warren, C. J., Grujic, D., Kellet, D. A., Cottle, J., Jamieson, R. A. & Ghalley, K. S. 2011. Probing the depths of the India-Asia collision: U-Th-Pb monazite chronology of granulites from NW Bhutan. *Tectonics*, **30**, 1–24.

Whitney, D. L., & Evans, B. W. 2010. Abbreviation for names of rock-forming minerals. *American Mineralogist*, **95**, 185–187.

Xu Z., Wang Q., Pêcher A., Liang F., Qi X., Cai Z, Li H., Zeng L. & Cao H. 2013. Orogen parallel ductile extension and extrusion of the Greater Himalaya in the late Oligocene and Miocene *Tectonics*, **32**, 191-215, doi: 10.1002/tec.20021.

Yakymchuk, C. J. A. & Godin, L. 2012. Coupled role of deformation and metamorphism in the construction of inverted metamorphic sequences: an example from farnorthwest Nepal. *Journal of Metamorphic Geology*, **30**, 513–535.

Yin, A. 2006. Cenozoic tectonic evolution of the Himalayan orogen as constrained by along-strike variation of structural geometry, exhumation history and foreland sedimentation. *Earth Science Reviews*, **76**, 1-131.

Figure captions

Figure 1. Schematic geological map of the Himalayan Belt. Numbered grey dots represent the location of the main tectonic and metamorphic discontinuities recognized along the belt: 1) Metamorphic discontinuity; Yakymchuk & Godin 2012; 2) Mangri Shear Zone; Montomoli *et al*. 2013; 3) Tojiem Shear Zone; Carosi *et al.* 2007, 2010; 4) Bhanuwa and Sinuwa Thrusts; Corrie & Kohn, 2011; Martin *et al.* 2010; 5) Himal Chuli; Larson *et al.* 2010, 2011; 6) Langtang Thrust; Fraser *et al.* 2000; Harris & Massey 1994; Kohn 2008; Kohn *et al.* 2005; Macfarlane 1993; Reddy *et al.* 1993; 7) Nyalam Thrust (Wang et al. 2013) 8) Tama Kosi; Larson 2012, Larson *et al.* 2013; Larson & Cottle 2014; 9) High Himal Thrust; Goscombe *et al.* 2006; Imayama *et al.* 2010, 2012; Hidden Discontinuity ; Groppo *et al.* 2009; 10) Age Discontinuity; Rubatto *et al.* 2012; 11) Bhutan Discontinuity; Swapp & Hollister 1991. SH: Siwalik Hills- Sub-Himalayan Molasse; LHS: Lesser Himalayan Sequence; GHS: Greater Himalayan Sequence; TSS: Tethyan Sedimentary Sequence; LH: Lhasa Batholith; HHL: High Himalayan Leucogranite; NHG: North Himalayan Leucogranite; GB: Gandgese Batholith; CG: Cretaceous Granite; MFT: Main Frontal Thrust; MBT: Main Boundary Thrust; STDS: South Tibetan Detachment System; MCT: Main Central Thrust; IYSZ: Indus Yarlung Suture Zone; KT: Karakorum Fault).

Figure 2. Representative meso and microstructures of HHD in Western Nepal (Mangri Shear Zone). a) Mylonitic paragneiss, with C-S fabric pointing to a top-to-the-SW sense of shear; b) Garnet bearing paragneiss with kinematic indicators (asymmetric rotated porphyroclasts, C-S fabric) showing a top-to-the-SW sense of shear; c) Composite sigmoidal mineral fish (*sensu* Mukherjee 2011) and mica fish; d) Chessboard extinction pattern in quartz indicating simultaneous prismatic and basal slip; e) Asymmetric strain shadows around garnet; f) Synkinematic growth of sillimanite on mylonitic foliation. (Mineral abbreviation after Whitney & Evans2010)

Figure 3. P-T conditions of samples from the HW (stars) and from FW (hexagons) from several tectonic discontinuities (see below) plotted on NKFMASH petrogenetic grid of Spear *et al.* 1999. Numbers as follows: 1) Yakymchuk & Godin 2012; 2) Montomoli *et al*. 2013; 3) Carosi *et al.* 2010; 4) Corrie & Kohn, 2011; 5) Larson *et al.* 2010; 6) Kohn 2008; 7) Larson *et al.* 2013, Larson & Cottle 2014; 8) Groppo *et al.* 2009; 9) Goscombe *et al.* 2006. See table 1 for more details and location of discontinuities.

Figure. 4. Sketch of the activity of the HHD (at 25-18 Ma) in the GHS at two different times and schematic examples of the P-T-paths of some rock in the HW (a1 and a2) and FW (b1 and b2) and possible trend of the isotherms perturbated by the contractional crustal-scale shear zone (modified after Kohn 2008, Nábělek & Nábělek , 2014 and reference therein). Point a (blue) is in the HW and point b (red) is in the FW of the HHD; t1: at the activation of the HHD point a1 exhumed whereas point b1 in the FW continued to undergo prograde metamorphism; t2: point a1 reached the position a2 with decreasing pressure and similar temperature caused by the possible contribution of shear heating in the shear zone; point b1 continued to be buried, reaching progressively higher pressure and temperature, until the activation time of the MCT, allowing the exhumation of the whole GHS. At the same time the rocks in the FW of the MCT (i.e. Lesser Himalaya) become incorporated in the orogenic prism and underwent prograde metamorphism.

Table 1. Summary table of the main tectono-metamorphic discontinuities recognized in the GHS in Central and Eastern Himalaya.

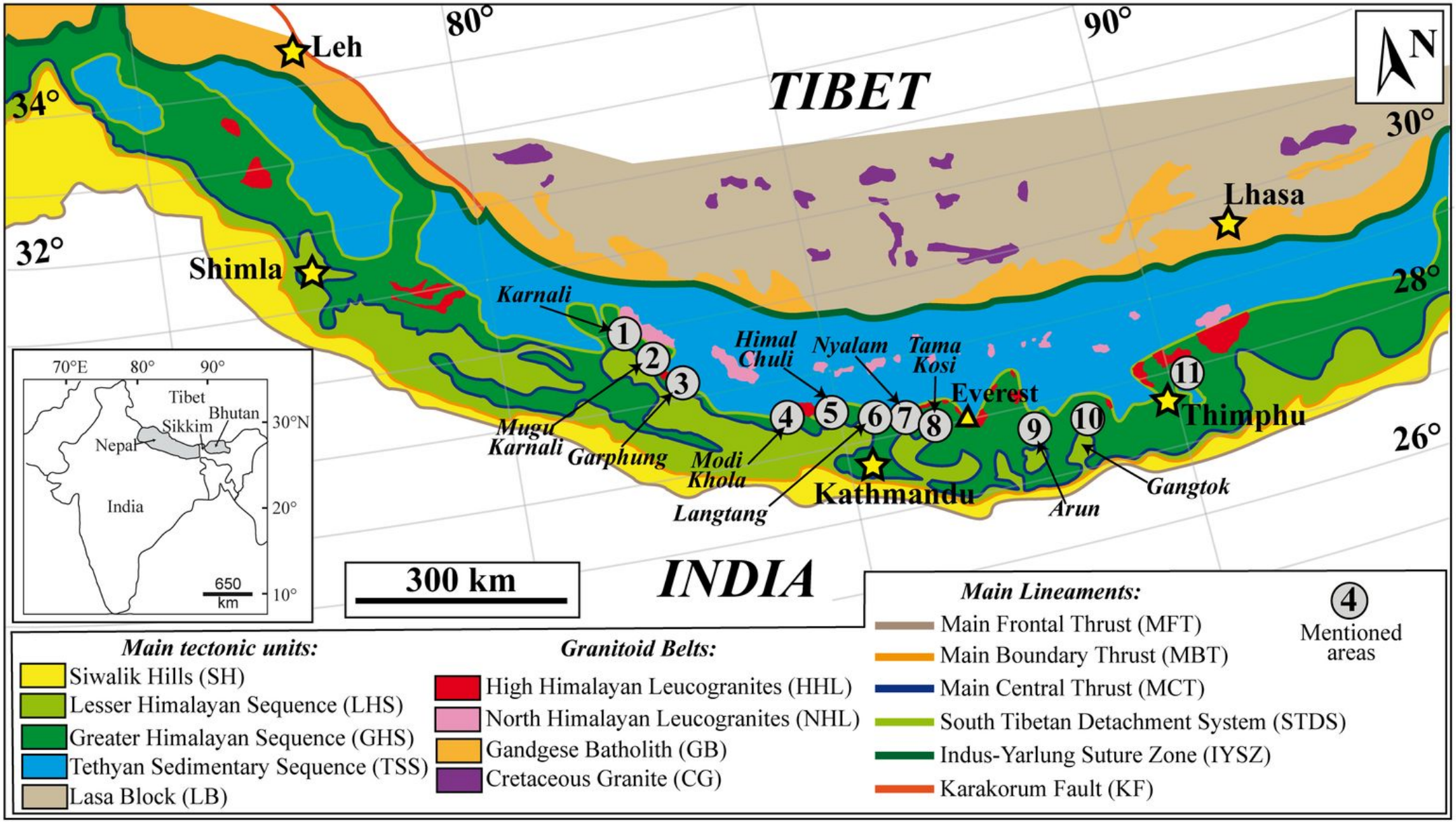
TIBET
INDIA
Leh
Shimla
Lhasa
Kathmandu
Thimphu
Everest
80°
90°
34°
32°
30°
28°
26°
N
Karnali
Mugu Karnali
Garphung
Modi Khola
Langtang
Himal Chuli
Nyalam
Tama Kosi
Arun
Gangtok
1
2
3
4
5
6
7
8
9
10
11
70°E
80°
90°
Tibet
Bhutan
Sikkim
Nepal
India
30°N
20°
10°
650 km
300 km
Main tectonic units:
Siwalik Hills (SH)
Lesser Himalayan Sequence (LHS)
Greater Himalayan Sequence (GHS)
Tethyan Sedimentary Sequence (TSS)
Lasa Block (LB)
Granitoid Belts:
High Himalayan Leucogranites (HHL)
North Himalayan Leucogranites (NHL)
Gandgese Batholith (GB)
Cretaceous Granite (CG)
Main Lineaments:
Main Frontal Thrust (MFT)
Main Boundary Thrust (MBT)
Main Central Thrust (MCT)
South Tibetan Detachment System (STDS)
Indus-Yarlung Suture Zone (IYSZ)
Karakorum Fault (KF)
4
Mentioned areas

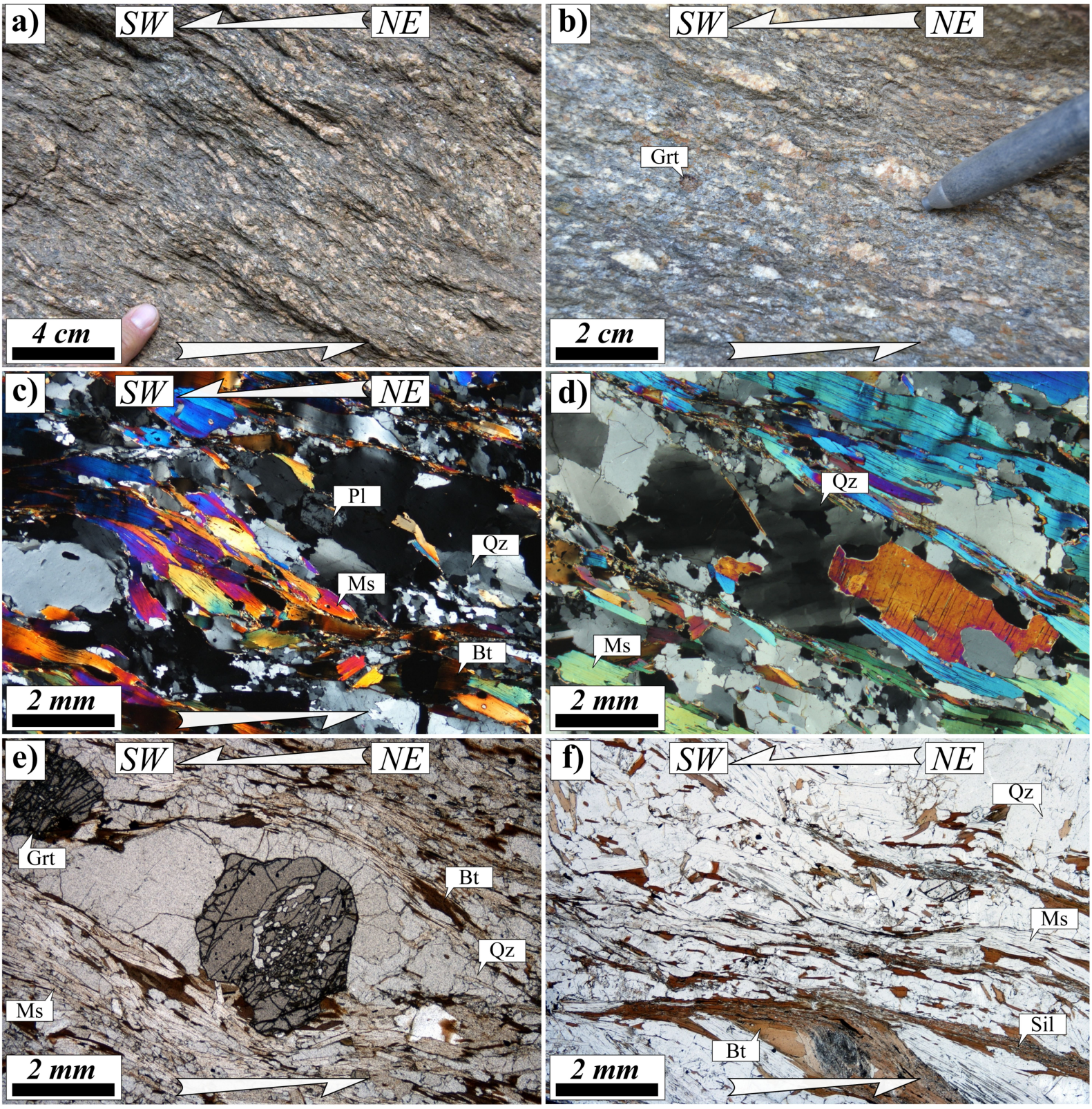
a)
SW
NE
4 cm
b)
SW
NE
Grt
2 cm
c)
SW
NE
Pl
Qz
Ms
Bt
2 mm
d)
Qz
Ms
2 mm
e)
SW
NE
Grt
Bt
Qz
Ms
2 mm
f)
SW
NE
Qz
Ms
Sil
Bt
2 mm

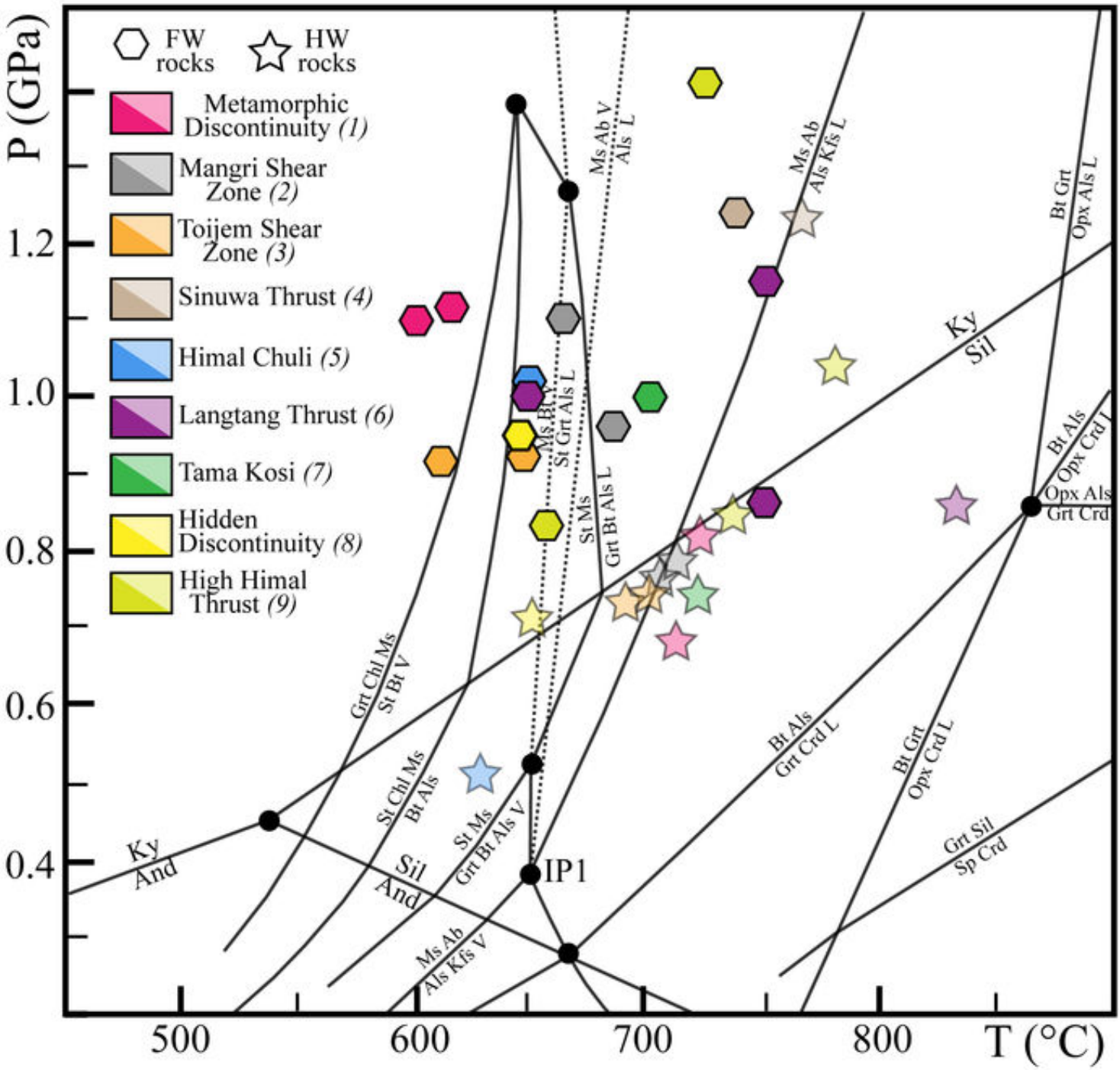
FW rocks
HW rocks
Metamorphic Discontinuity (1)
Mangri Shear Zone (2)
Toijem Shear Zone (3)
Sinuwa Thrust (4)
Himal Chuli (5)
Langtang Thrust (6)
Tama Kosi (7)
Hidden Discontinuity (8)
High Himal Thrust (9)
P (GPa)
1.2
1.0
0.8
0.6
0.4
500
600
700
800
T (°C)
Ky
And
Sil
And
Ky
Sil
IP1
Grt Chl Ms
St Bt V
St Chl Ms
Bt Als
St Ms
Grt Bt Als V
Ms Ab
Als Kfs V
Ms Bt
St Grt Als L
St Ms
Grt Bt Als L
Ms Ab V
Als L
Ms Ab
Als Kfs L
Bt Als
Grt Crd L
Bt Grt
Opx Crd L
Grt Sil
Sp Crd
Bt Grt
Opx Als L
Bt Als
Opx Crd L
Opx Als
Grt Crd

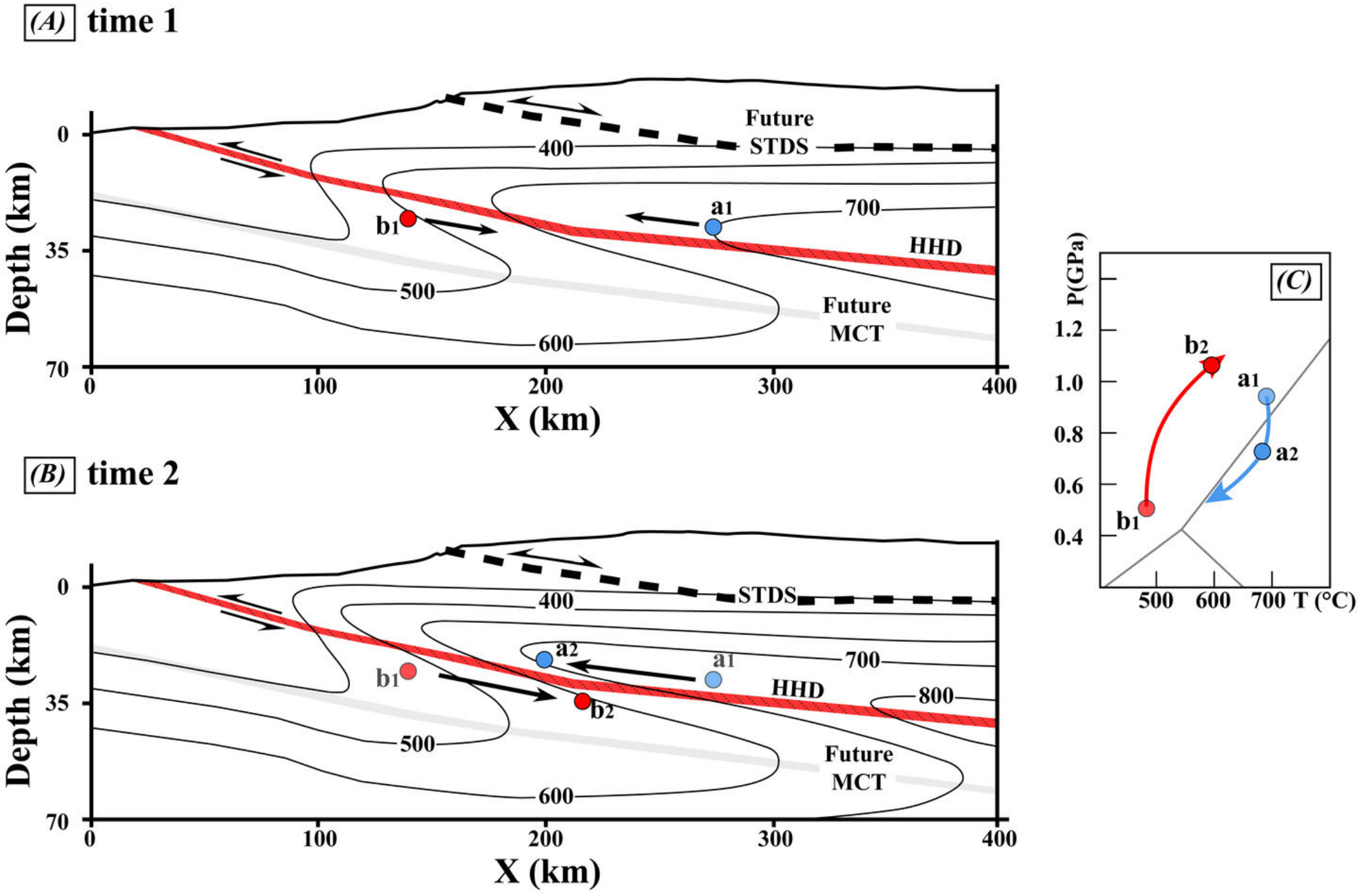
(A) time 1
Future
STDS
400
700
a1
b1
HHD
500
Future
MCT
600
Depth (km)
0
35
70
0
100
200
300
400
X (km)
(B) time 2
STDS
400
a2
a1
700
b1
HHD
800
b2
500
Future
MCT
600
Depth (km)
0
35
70
0
100
200
300
400
X (km)
(C)
P(GPa)
1.2
1.0
0.8
0.6
0.4
b2
a1
a2
b1
500
600
700
T (°C)

Table 1. *Main features of tectono-metamorphic discontinuities within the GHS along Central-Eastern Himalaya (from Western, Central and Eastern Nepal, Sikkim and Buthan).*

Name	Locality	Metamorphic rocks		P-T estimate		Timing of activity	References	Age of MCT
		Footwall	Hanging wall	Footwall	Hanging wall			
Metamorphic Discontinuity (MD)	Karnali valley (Western Nepal)	St/Ky-bearing metapelites	Ky/Sil-bearing migmatitic para/orthogneiss	~1.1 GPa 600-630 °C	~0.6-0.8 GPa 650-720 °C	–	Yakymchuk & Godin (2012)	–
Mangri Shear Zone (MSZ)	Mugu Karnali (Western Nepal)	St/Ky±Sil-bearing paragneiss & orthogneiss locally anatectic	Sil+Ms/Kfs-bearing gneiss & migmatites	~0.9-1.1 GPa 650-700 °C	~0.7-0.8 GPa 690-720 °C	25-18 Ma (U-Th-Pb, Mnz)	Montomoli *et al.* (2013)	17-13 Ma (Montomoli et al., 2013)
Toijem Shear Zone (TSZ)	Garphung Khola (Western Nepal)	Ky-bearing metapelites	Sil-bearing and migmatitic gneiss	~0.9 GPa 600-650 °C	~0.7 GPa 675-700 °C	26-17 Ma (U-Th-Pb,	Carosi *et al.* (2007, 2010)	22-10 Ma (De Celles et al., 2001)
Sinuwa Thrust (ST)	Modi Khola valley (Central Nepal)	Ky-bearing metapelites, locally anatectic	Ky-bearing migmatites	~1.25 GPa 735 °C	~1.25 GPa 775 °C	27-22 Ma (Th-Pb, Mnz)	Corrie & Kohn (2011) Nadin & Martin (2012)	22-13 Ma (Catlos et al. 2004)
P-T-t-D (Himal Chuli)	Himal Chuli (West-Central Nepal)	St/Ky-bearing metapelites & orthogneiss	Sil-bearing anatectic paragneiss	~0.9-1.1 GPa ~600-650 °C	~0.5-0.4 GPa ~610-640 °C	23-15 Ma (U-Th-Pb, Mnz)	Larson *et al*. (2010, 2011) Kohn *et al*. (2001)	21-8 Ma (Kohn et al. 2004)
Langtang Thrust (LT)	Langtang region (Central Nepal)	Sil+Ms/Ky-bearing migmatitic gneiss	Sil+Kfs-bearing migmatitic gneiss	~0.85-1.15 GPa 650-750 °C	~0.85 GP 825 °C	21-19 Ma (Th-Pb, Mnz)	Kohn *et al*. (2004, 2005) Kohn (2008)	16-9 Ma (Kohn et al. 2004)
P-T-t-D (Tama Kosi)	Tama Kosi (Eastern-Central Nepal)	Ky/Sil-bearing migmatitc paragneiss	Sil-bearing migmatitc paragneiss	~1.0 GPa ~700-725 °C	~~0.71-0-77 GPa ~7020-750 °C	< 22 Ma (U-Th-Pb, Mnz)	Larson & Cottle (2014)	19-15 Ma (Larson et al. 2013)
"Hidden Discontinuty " (HD)	Arun tectonic window (Eastern Nepal)	St/Ky-bearing subsolidus rocks	Ky/Sil-bearing subsolidus to suprasolidus rocks	~0.85-0.95 GPa 600-650 °C	~0.75-1.0 GPa 655- ~800 °C	–	Groppo *et al.* (2009)	–
High Himal Thrust (HHT)*	Tamor-Ghunsa (Far-Eastern Nepal)	St/Ky-bearing gneiss Sil+Ms migmatites	Sil+Kfs ± Crd migmatites	~0.8-1.4 GPa ~780 °C	~0.7-1.0 GPa 730-780 °C	27-23 Ma (U-Pb, Zrn)	Goscombe *et al.* (2006) Imayama *et al.* (2010, 2012)	22-13 Ma (Goscombe et al. 2006)
"Age discontinuity"	Sikkim	Sil+Kfs±Crd migmatites	Sil+Kfs±Crd migmatites with Ky relicts	~0.8 GPa 750-850 °C	~0.9 GPa 750-850 °C	23-20 Ma (U-Pb, Mnz/Zrn)	Rubatto *et al.* (2012)	22-13 Ma (Catlos et al. 2004)
Modi Khola Shear Zone (MKSZ) #	Modi Khola valley (Central Nepal)	Grt/Ky-bearing gneiss and calcsilicate	Amphibolite grade calcsilicate and orthogneiss	–	–	22.5-18.5 Ma (U-Pb, Zrn)	Hodges *et al*. (1996)	22.5 Ma (Hodges et al. 1996)
Nyalam Thrust (NT) #	Nyalam region	Ky/Sil-bearing non migmatized paragneiss	Sil/Crd- bearing migmatitic gneiss	1.2 up to 0.39 GPa 630-670 °C	0.69 up to 0.41 GPa 705-750°C	< 14 Ma (U-Pb Zrn)	Wang et al., 2013	21 Ma (Viskupic et al. 2005) 23-23-20 Ma (Hubbard 1989)
Laya Thrust (LT) #	NW-Bhutan	amphibolite grade rocks	granulazied eclogites bearing	0.6-0.8 GPa 600-650 C°	0.8-1.0 GPa 750-800 °C	~15-13 Ma (U-Pb, Mnz)	Grujic *et al.* (2002, 2012) Warren *et al.* (2011)	20-15 Ma (Tobgay et al. 2012)
Kakhtang Thrust (KT) #	NE-Bhutan	St/Ky±Sil-bearing para-orthogneiss locally anatectic	Ky/Sil+Kfs±Crd-bearing migmatites	0.6-1.3 GPa 600-640 °C	~0.9 GPa 700-720 C°	15-10 Ma (U-Pb, Mnz)	Davidson *et al.* (1997) Grujic *et al.* (1996, 2002) Daniel *et al.* (2003) Long & McQuarrie (2010) Chambers *et al.* (2011)	23-20 Ma (Tobgay et al. 2012) 18-13 Ma (Daniel et al., 2003)
Buthan Thrust #	N Bhutan	St/Ky±Sil-bearing paragneiss	Sil+Kfs±Crd-bearing migmatites	~0.7 GPa 480-500 °C	~0.4 GPa 630 C°	–	Swapp & Hollister (1991)	

* normal fault reactivation at 18–16 Ma (U-Pb, Zrn) # Out of Sequence Thrusts